PROCEEDINGS, Twelfth Workshop on Geothermal Reservoir Engineering
Stanford University, Stanford, California, January 20-22, 1987
SGP-TR-109

GEOCHEMISTRY AND TRACER BEHAVIOR DURING A THIRTY DAY FLOW TEST OF THE FENTON HILL HDR RESERVOIR

Bruce A. Robinson, Ronald G. Aguilar, Yuji Kanaori,
Pat Trujillo, Dale Counce, Stephen A. Birdsell and Isao Matsunaga

Los Alamos National Laboratory
Los Alamos, New Mexico 87545

ABSTRACT

During the most recent circulating flow test of the Fenton Hill Hot Dry Rock (HDR) geothermal reservoir, the geochemical behavior of the produced fluid was monitored continuously to determine the concentrations of dissolved anions and cations and dissolved gases. Chemistry results have aided in the development of reservoir models and in the determination of potential chemistry-related operation problems such as corrosion and gas handling in future energy extraction tests. Results of two radioactive tracer experiments suggest flow through a large, highly-fractured region of rock. This rock volume is equivalent to a sphere of diameter approximately equal to the separation distance between the injection and production points in the two wells.

INTRODUCTION

A 30-day closed-loop circulation test of the current HDR reservoir at Fenton Hill, NM has been performed to determine the hydraulic, seismic, and chemical characteristics of the reservoir, in anticipation of a long-term energy extraction test scheduled to start in January 1988. Hendron (1987) summarized this flow test, focusing on the overall reservoir performance. The present study examines the geochemistry and tracer results obtained from continuous sampling of the production fluid and the injection of radioactive tracers to measure fracture volumes and dispersive characteristics.

GEOCHEMISTRY OF THE FLOW TEST

GEOCHEMISTRY DATA

Sampling Apparatus and Procedures: The apparatus used to collect produced fluid gas and liquid samples is shown in Figure 1. Hot, pressurized fluid from a sidestream off the production wellhead flowed to a small chemistry laboratory containing this equipment. The fluid was cooled under pressure in a heat exchanger and directed to the various apparatus in the figure either manually or automatically, depending on the sample being collected. Filtered and unfiltered liquid samples were collected manually through

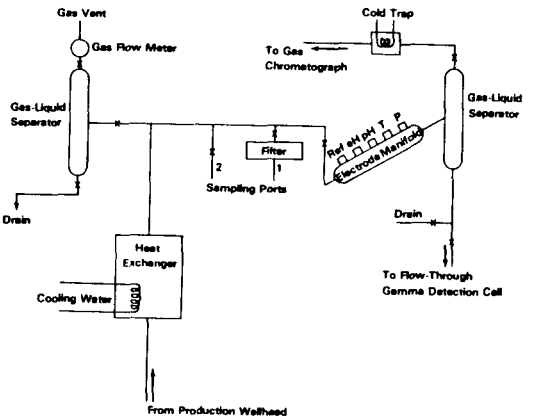

Figure 1. Schematic of the sampling apparatus for production fluid liquids and gases.

the ports labeled 1 and 2. Alternatively, fluid passed through an instrumented manifold kept at a pressure sufficient to prevent degassing. The eH, pH, and electrical conductivity of the fluid were recorded automatically in this manifold. The gas separation equipment on the right side of the figure supplied gas samples for the gas chromatographic and radon analyses. This separator was operated continuously, with gas samples directed periodically to the gas chromatograph after passing through a cold trap to remove any remaining moisture. In addition, the liquid effluent from this separator was directed to the gamma counter during the radioactive tracer experiments.

The other gas separation unit was used to simultaneously measure gas and liquid flow rates to obtain the gas mass fraction in the produced fluid. The separator was manually adjusted to achieve a constant liquid level and gas flow rate, and the gas and liquid flow

rates were measured simultaneously. Since the gas was predominantly CO_2, the concentration of CO_2 (in weight percent) in the produced fluid was determined directly.

The procedures employed at Fenton Hill for analyzing gas and liquid samples for dissolved anions, cations, gas concentrations, suspended solids, and other species is described in detail elsewhere (Trujillo et al., 1986).

Major Dissolved Species: Figure 2 shows the concentration-time behavior of the major dissolved anions and cations in the produced fluid. Table 1 shows the concentrations in a sample collected six days into the flow test, after the geochemical behavior had reached a quasi-steady state. The concentrations of most species are 2-3 times higher than in previous shallower reservoirs, probably because of higher reservoir temperatures and a larger contribution from the in situ pore fluid. The total dissolved solids value of 4300 ppm, equivalent to ionic strength I = 0.05 m, is low enough that major brine handling problems are not expected.

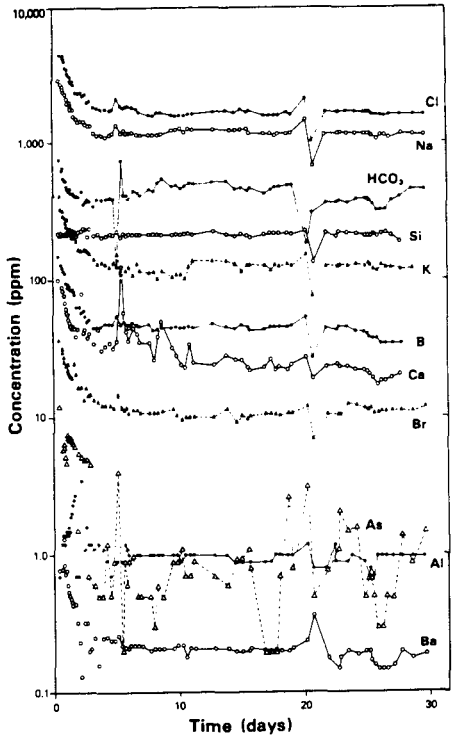

Figure 2. Concentration-time behavior of the major dissolved species in the production fluid.

Non-Condensable Gas Analyses: Gas analysis consisted of total gas flow rate (Figure 3) and gas chromatograph analysis of the dry gas composition. After the initial transient in the first few days of the flow test, the average gas flow rate was about 0.2% CO_2 by weight. Dismissing the high gas flow rates during a nitrogen injection experiment on day 20, the highest values were observed during the experiment start-up. The high value of 0.9% is the best estimate of the CO_2 concentration in the pore fluid. Higher gas concentrations may have been present during periods of two-phase flow, but our sampling apparatus did not enable us to obtain a representative sample of the fluid during two-phase flow.

Gas chromatograph analyses determined the dry gas to be predominantly CO_2 (typically 90-95%), with lesser quantities of N_2, and minute amounts of H_2S, O_2, and occasionally CH_4 and C_2H_6.

Table 1.

Typical Ion Concentrations (Sample Collected on Day 6)

Component	Concentration (ppm)
As	0.6
B	48
Br	11.5
Ca	42
Cl	1814
F	10.4
Fe	2.1
HCO_3	408
K	114
Li	23.4
Na	1180
pH	5.79
SiO_2	452
SO_4	183
TDS	4300 (I = 0.05m)

INTERPRETATION OF GEOCHEMISTRY

Time-Dependent Behavior: When fluid of different concentration than the underground pore fluid is injected into a circulating HDR reservoir, the resulting produced fluid geochemistry behavior will be governed by three mechanisms: 1) displacement of the downhole fluid by the injected water, 2) rock-water dissolution, precipitation, or alteration reactions, and 3) adsorption of chemical species on the reservoir rock. Throughout most of the flow test, the downhole, injection, and makeup fluids were all at similar concentrations (approximately those listed in

Table 1). However, early in the test the inlet and outlet concentrations were different, and can be interpreted most effectively by defining a non-dimensional concentration C* (Grigsby, 1983):

$$C^* = \frac{C - C_{in}}{C_o - C_{in}} \quad (1)$$

where C_{in} is the injection concentration and C_o is the initial produced fluid concentration, which is the true downhole concentration of the component if the sample is collected immediately after the wellbore fluid is displaced. The most common behavior is that of

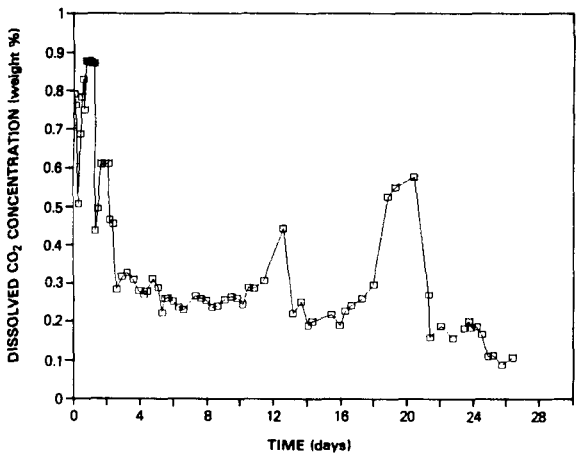

Figure 3. Dissolved CO_2 concentration in the production fluid.

an inert, nonadsorbing species, which behaves like a tracer for a negative step change in injection concentration. Injected fluid gradually sweeps the concentrated underground pore fluid from the reservoir until the produced fluid concentrations approach the injection values (Figure 4). Chloride ion, Cl, as well as B, Br, K, Li, Na, electrical conductivity, and total dissolved solids all fall in this category.

Two other characteristic concentration-time responses are exhibited in Figure 5. The dissolved silica concentration remained constant during the initial sweep of pore fluid from the reservoir and throughout the entire 30 day test. Quartz dissolution supplies a constant source of silica to the undersaturated injection fluid, allowing the solution to reach equilibrium in one pass through the reservoir. The third type of time-dependent behavior is for species whose concentration decreases to a value below the injection value. This result implies consumption of the component, either by adsorption on the rock surface or precipi-

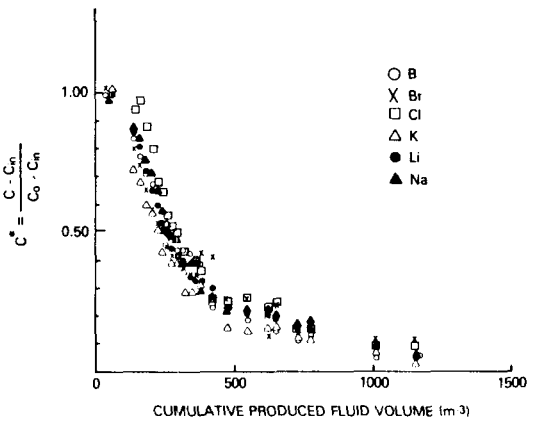

Figure 4. Dimensionless concentration versus produced fluid volume for inert species during initial reservoir operation. Concentrations start at high downhole values and decline to injection fluid concentration.

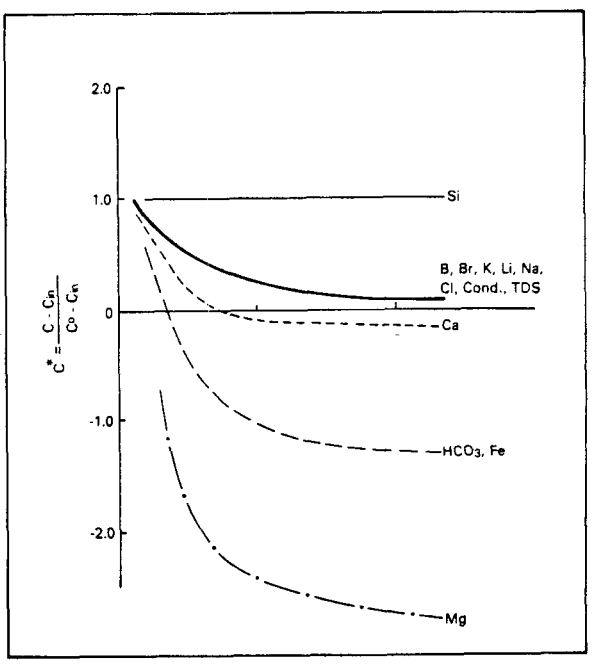

Figure 5. Different types of concentration-volume behavior observed during initial reservoir operation.

tation reactions. Divalent cations such as Mg clearly show a propensity to adsorb on granite, and, as shown in the figure, fall into this third category. Calcium, bicarbon

ate, and iron also exhibit this behavior, though the mechanisms for these three components are as yet unclear. Finally, a few species such as Ba, Mn, and SO_4 exhibit anomalous time dependences which have not been explained.

Sources of Dissolved Species: The origin of dissolved species in hot dry rock geothermal fluids has been treated by Grigsby et al. (1983). The two primary sources of dissolved species are displacement of downhole pore fluid and dissolution of minerals. Current models postulate a continuous extraction of the original pore fluid from the fractured rock mass over long periods of time. The most compelling argument supporting this theory is the presence and continued supply of chemically inert species such as boron and chloride, which are not found in the reservoir granite and hence are not supplied by a dissolution reaction.

Since most reservoir fluid samples are composed of the original downhole fluid after dilution with injected fluid, true values of the pore fluid concentrations are difficult to obtain. Grigsby (1983) has demonstrated that even when the pore fluid is diluted, the ratios of ions in solution should remain constant for conservative species supplied only by pore fluid, rather than by mineral

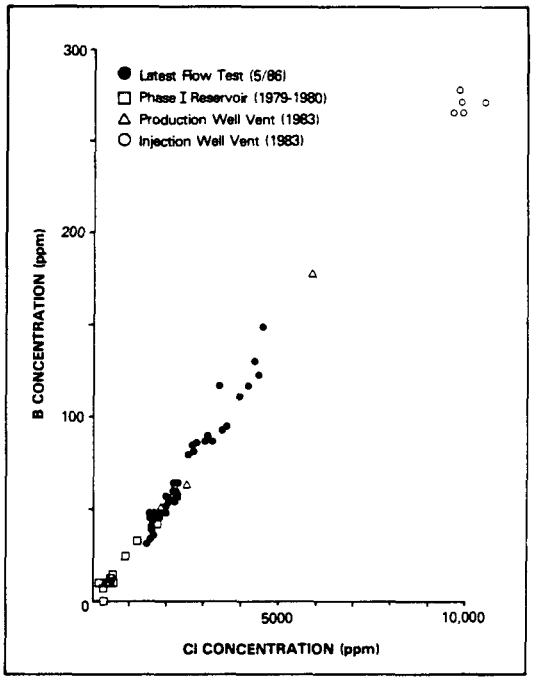

Figure 6. B versus Cl for fluid samples collected in the Fenton Hill HDR reservoir over the past eight years.

dissolution or alteration. When the concentration of one component is plotted directly against another, the data should fall on a single straight line if the source of the pore fluid is the same. Figure 6 is a plot of B versus Cl for the latest flow test and previous Fenton Hill circulation experiments and events of the past eight years. The new data all fall on the same straight lines as those for other fluid samples collected at Fenton Hill. The evidence now even more strongly supports the pore fluid hypothesis and suggests that a single underground fluid supplies the conservative species found in fluid samples at the Fenton Hill site.

Rock-water reactions are also important in the production or consumption of some species. For example, quartz dissolution controls the concentration of dissolved silica in the production fluid. The constant concentration measured during the flow test implies that the kinetics of quartz dissolution were rapid enough for the fluid to reach saturation in one pass through the system. Robinson (1982) measured the rate of quartz dissolution as a function of temperature and rock surface area and determined the following relation:

$$\ln \Phi = \ln \left[\frac{C^{\infty} - C}{C^{\infty} - C_{in}}\right] = -ka^{*}t \qquad (2)$$

where a* is the quartz surface area to fluid volume ratio ($2f_q/b$ for a flat fracture, where b is the fracture aperture and f_q is the fraction of quartz present in the granite), C^{∞} is the saturation concentration, and k is the rate constant for dissolution. To obtain a minimum value for a*, or a maximum value for the average fracture aperture, the following values will be used:

- Φ = 0.1 (equivalent to the dissolution reaction reaching 90% of its equilibrium value)
- t = 10 hr (the residence time at the peak tracer response)
- k = 4.13×10^{-8} m/s at 250°C (Robinson, 1982)
- f_q = 0.3

These assumptions yield a* = 1550 m^{-1}, or b = 0.4 mm. In other words, the average aperture encountered by fluid should be no greater than about 0.4 mm, and quite possibly less in order for the system to reach saturation with respect to quartz in one pass through the reservoir. Future models for the permeability and tracer behavior of the reservoir must be consistent with this information.

Another set of reactions affecting the produced fluid chemistry is the dissolved carbon dioxide-bicarbonate equilibrium reactions, which are coupled to the calcite dissolution reaction. Carbon dioxide is present in the underground pore fluid and is produced along with other pore fluid elements. If calcite (calcium carbonate, $CaCO_3$) is present, its solubility is also affected by the presence of

dissolved CO_2. For a CO_2-rich fluid in equilibrium with calcite, the following chemical reaction applies:

$$CaCO_3 + H_2O + CO_{2(g)} \rightleftharpoons Ca^{2+} + 2HCO_3^- \quad (3)$$

with equilibrium constant K_{eq} equal to

$$K_{eq} \frac{\gamma_{Ca}\,\gamma^2_{HCO_3}\,[Ca][HCO_3]^2}{P_{CO_2}} \quad (4)$$

The concentrations are in mol/l, the γ's, the activity coefficients, are related to ionic strength and temperature using the Debye-Huckel equation (Henley et al., 1984) and P_{CO_2}, the partial pressure of CO_2 is given by

$$P_{CO_2} = K_H\, x_{CO_2} \quad (5)$$

where K_H, the Henry's law constant for CO_2, is a function of temperature, and x_{CO_2} is the fraction of CO_2 in the liquid. Using the measured values of all concentrations, and expressions supplied by Henley et al. (1984) for K_H and the γ's, we may iteratively calculate the equilibrium temperature at which these dissolved species were produced. For the 75 samples analyzed, the average calculated temperature was 211°C, with a standard deviation of 16°C. These temperatures are in reasonable agreement with the measured downhole production temperature of about 232°C, suggesting that for a given downhole P_{CO_2}, calcite dissolution is governing the equilibrium between dissolved CO_2, bicarbonate ion, and Ca. As significant changes in downhole temperatures occur due to thermal drawdown or exposure of hotter fluid flow paths, corresponding changes in these concentrations should also occur. However, to use these equilibrium reactions to evaluate reservoir temperature patterns, further refinements of the calculations will be required to explain the 20°C discrepancy between the actual and average calculated temperatures.

Geothermometer Readings: Since rock-mineral dissolution or alteration reactions are temperature dependent, the concentrations of certain dissolved species will depend on temperature. The calculations just presented are one example. Two more commonly used chemical geothermometers which exploit this temperature sensitivity are the quartz and Na-K-Ca geothermometers. These two measurements are shown for samples collected throughout the flow test in Figure 7. The recorded geothermometer temperature for quartz dissolution of about 250°C agrees fairly closely with the actual downhole temperature. The reactions governing the Na-K-Ca geothermometer do not reach equilibrium in short times, however. Thus, since the produced fluid is a mixture of the injection fluid and underground pore fluid, these geothermometer readings are not as precise. The Na-K-Ca temperatures decrease from essentially the known rock temperature to a somewhat lower value. In future work we will model this behavior, as well as the carbon dioxide-bicarbonate equilibrium reactions, as the mixing of fluids of different concentrations and temperatures to attempt to determine what concentrations and flow fractions are required to match the results.

CHEMICAL EFFECTS ON OPERATIONS

Corrosion Studies: Due to the large number of metal hardware failures attributed to metallic corrosion during the drilling of the injection and production wellbores, corrosion monitoring was performed during this flow test. Of greatest concern are the high temperatures, gas concentrations, and concentrations of corrosive ions such as Cl^-. This one month flow test provided data for future surface loop design.

Corrosion coupons were placed on side streams off the mainstream flow on both the hot and cold sides of the heat exchanger. Each station contained two coupons attached to a coupon holder of sufficient length that the coupons were exposed to a representative sample of the fluid. The coupons were oriented parallel to the fluid flow to avoid possible corrosion due to erosion. Shutoff valves placed at both stations allowed the coupons to be removed periodically. Pressure taps were placed at the entrance and exit

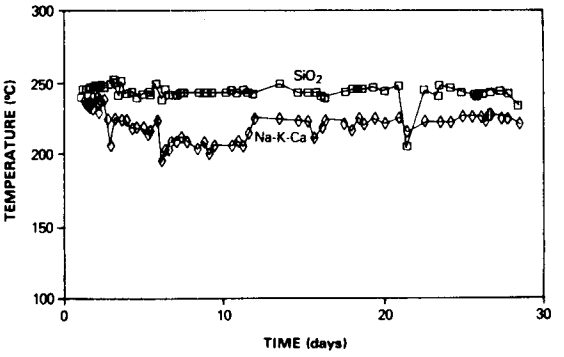

Figure 7. Silica and Na-K-Ca geothermometer temperatures.

points of the side stream piping to direct the fluid flow to the coupons. The coupons were analyzed periodically for corrosion rate (by measuring coupon weight loss over a specified time, typically 150 hr), type of corrosion, and scale formation.

The corrosion rates at various times during the flow test are presented in Figure 8. The more rapid corrosion rates occurring on the hot side of the heat exchanger are due to the

increased temperature, which increases the attack of metal hardware by elemental species present in the production fluid. The highest corrosion rate of 15 mils per year (mpy), occurring with the second set of coupons, will be used as the design criterion for the surface equipment for future tests. In the final set of coupons, the hot-side corrosion rate decreased dramatically. We attribute this result to equipment malfunctions which prevented liquid flow from reaching the coupons.

The type of corrosion observed on both sample stations was generalized and uniform. This behavior is typical of metal exposed to acidic fluid under flowing conditions. The only deviation from this pattern was in the final set of coupons on the cold side, where the corrosion rate increased and extensive pitting was observed. This anomalous behavior is probably due to the increase in dissolved oxygen observed at this time.

When assessing the potential for corrosion damage in geothermal systems, the type of corrosion is more important than the rate of metal dissolution. A high concentration of Cl^- or dissolved O_2 induces pitting, which increases potential equipment failures dramatically. The lack of heavy pitting on our corrosion coupons suggests that materials will not be subjected to severe corrosive attack. Nonetheless, surface hardware durability and performance in future flow tests can be enhanced with appropriate corrosion treatment. Alternatively, corrosion-resistant materials or heavy-walled pipe could be used, but in our

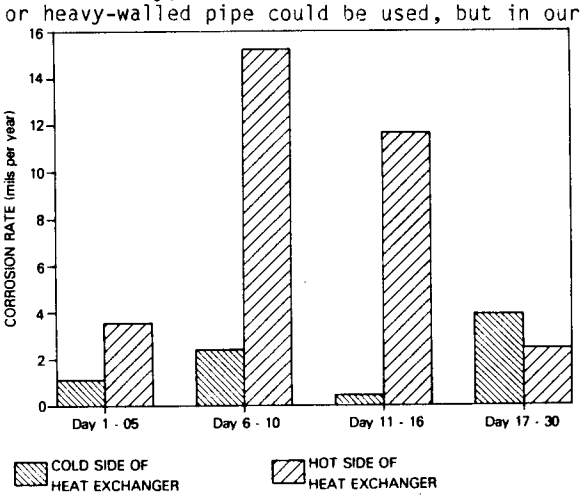

Figure 8. Corrosion rates measured on the hot and cold sides of the heat exchanger. Each value is obtained from a weight loss determination for a coupon exposed to fluid during the times labelled.

case the cost advantages of light carbon steel equipment outweigh the possible benefits of these approaches, particularly if dissolved gases are handled properly. To minimize corrosion during longer periods of operation, dissolved oxygen in the injection fluid will be kept low (in the parts per billion range) by injecting an oxygen scavenger such as ammonium bisulfite or hydrazine.

Gas Handling: To keep a geothermal fluid containing dissolved CO_2 single-phase, the total system pressure must be greater than the sum of the partial pressures of CO_2 and water:

$$P > P_{CO_2} + P_W \qquad (6)$$

This expression is valid for a closed system not open to the atmosphere. The partial pressure of water, P_W, is approximately equal to its vapor pressure. The term P_{CO_2} is a function of the concentration of CO_2 in the liquid phase and its Henry's law constant K_H, as given by Eqn. (5). The constant K_H and P_W are both functions of temperature. Figure 9 shows the minimum pressure required to keep the solution a single phase liquid for different temperatures and concentrations of dissolved CO_2.

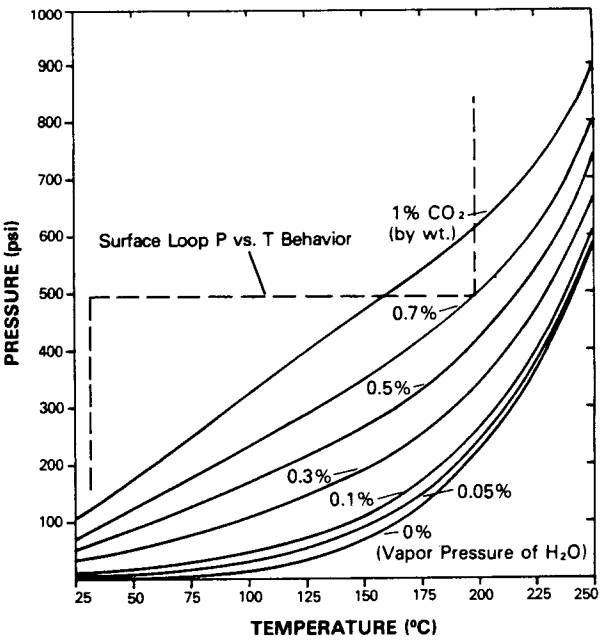

Figure 9. Pressure required to keep a CO_2 - H_2O solution single-phase for different CO_2 concentrations and temperatures. Dotted line is a typical (P,T) curve for an element of fluid passing through the surface loop equipment.

During most of the flow test, dissolved CO_2 remained in the liquid phase and was reinjected after energy extraction. A simple calculation or use of Figure 9 shows why this was possible.

The dotted line in Figure 9, representing the pressure-temperature behavior of fluid in the surface loop, shows that only fluids with dissolved CO_2 concentrations greater than 0.7% will cause flashing. For the typical value of 0.2 - 0.3%, mixture will remain a single phase. Occasionally, new regions of the reservoir were accessed and a transient period of high CO_2 concentration occurred. Phase separation in the production wellbore prevented us from collecting a representative sample, but Figure 9 shows that the CO_2 concentration must have been about 1% or greater. For future operations we will install a high pressure, high temperature gas separator to handle these occasional gas surges.

Scale Deposition: The two types of scale deposition which were of greatest concern before the flow test were silica and calcite precipitation. When water saturated with respect to quartz at reservoir temperatures is cooled, it becomes supersaturated with respect to all forms of silica. Hence a driving force for silica scaling is present. Calcite precipitation occurs for a different reason. Flashing of CO_2 from solution creates disequilibrium which, according to elementary chemical thermodynamics, will cause the reaction of Eqn. (3) to proceed to the left to reachieve equilibrium. Thus, calcite ($CaCO_3$) is deposited.

Despite these potential mechanisms, very little scale deposition was uncovered in a post-experiment examination of the surface loop, and this scale did not adversely affect the performance of the equipment. Only a small amount of calcium carbonate scale was found on a pipe leading to the heat exchanger, while no silica deposits were found. However, some magnetite scale was detected in the inlet manifolds of the heat exchangers, although we cannot determine whether it was deposited during this or a previous flow test. In addition, a yellowish precipitate containing about 4% arsenic was detected on the corrosion coupons on the cold station of the heat exchanger and in the heat exchanger itself.

RADIOACTIVE TRACER EXPERIMENTS

PROCEDURES

Two radioactive tracer experiments, the first on day 10 and the second on day 25, were carried out using an irradiated form of the water soluble salt, ammonium bromide, NH_4Br. The tracer, ^{82}Br, a gamma-emitting radionuclide with a half-life of 35.3 hr, has been used as a conservative (nonreacting, nonadsorbing) tracer at Fenton Hill for several years (Robinson and Tester, 1984). In each tracer experiment a sample was irradiated in Los Alamos's Omega West nuclear reactor, assayed, and transported to the Fenton Hill site. Accounting for radioactive decay during the transportation, the injected pulse strengths were 61.9 mCi and 70.2 mCi. Measurements of gamma activity as a function of time were obtained in the mobile chemistry laboratory by flowing a liquid sidestream through a continuous flow cell equipped with a NaI scintillation counter.

RESULTS

To obtain a residence time distribution (RTD) curve from a pulse injection tracer experiment, the background radioactivity must be subtracted and the resulting value corrected for radioactive decay. Then, the RTD f(V) is given by

$$f(V)= \frac{C(V)}{m_p} \qquad (7)$$

where C(V) is the corrected concentration at produced fluid volume V, and m_p is the mass of the tracer pulse.

When the produced fluid is recirculated, as in the first test, the concentration-time response must also be corrected for the reinjection of radioactive fluid using a mathematical deconvolution technique (Robinson and Tester, 1984). This calculation was performed for the first experiment, while the second test was conducted in the open loop injection mode with production fluid returns temporarily vented to a holding pond. Thus in the second test the true RTD was obtained directly from Eqn. (7).

The RTD curves for the two experiments are shown in Figure 10. The most striking difference from tracer tests in past Fenton Hill reservoirs is the low recovery of tracer. The ^{82}Br tracer experiment is limited to 2-3 days due to its half-life, so the low tracer recoveries actually imply that a larger percentage of the fluid has residence times longer than 3 days. According to current models of tracer flow through fractured reservoirs, the present system must contain flow paths of large volume which conduct at least half the fluid. In addition, the modal volume (produced fluid volume at the peak of the response curve), a standard correlating parameter for estimating the heat transfer capacity of a fractured HDR reservoir, (Robinson and Tester, 1984) is larger by roughly a factor of two than previous Fenton Hill reservoirs at a similar stage of operation. Hence we expect a longer-lasting reservoir with more gradual production fluid temperature drawdown than in the past.

Comparing the two tracer curves, the response is shifted to larger volumes, and less tracer was recovered in the second test. This result is due to the transient state of the reservoir during the flow test - throughout the test, the difference of the inlet and outlet flow rates, commonly thought of as water loss, was in large part going into charging the reservoir. Thus a dramatic increase in the integral mean volume (the volume of all fractures connecting the two wellbores, re-

gardless of residence time) from 2180 to 8440 m^3 was observed. The post-experiment vent of the reservoir supports the idea that the observed water loss was caused by the need to fill the fracture system. Of the total of 12000 m^3 net water lost to the fracture system, 6400 m^3 has returned during the vent. Both of these values are rough agreement with the fracture volume of 8440 m^3 measured in the second tracer test.

The fracture volume estimates aid in the development of conceptual models of the flow system. Assuming a homogeneous fracture network of known porosity, fracture volumes may be used to calculate the swept rock volume. The value of fracture porosity may be bounded between 0.0002 - 0.001, based measurements of seismicity and reservoir compressibility calculations. For a fracture porosity of 0.001, the rock volumes calculated from the two tracer experiments correspond to a sphere of diameter 160 m for the first and 250 m for the second. Although the value of porosity is inexact, the resulting sphere diameters are of the same order of magnitude as the wellbore separation distance of 110 m. Thus the conceptual model of flow through a large network of fractures with a point source and sink is a reasonable first approximation.

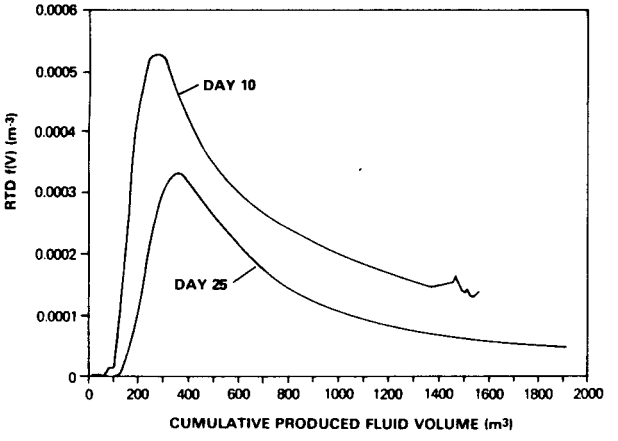

Figure 10. Residence time distribution curves obtained from the two radioactive tracer experiments.

CONCLUSIONS

1. The geochemistry of the production fluid over the first 5 days of the experiment followed three characteristic trends: 1) the decline of inert species from their initial concentrations to the injection fluid concentration; 2) no change in concentration, indicating a supply of the dissolved species via dissolution reactions (SiO_2); 3) and decline of concentration to below the injection concentration, caused by absorption, precipitation, or ion exchange reactions.
2. The Na-K-Ca and SiO_2 geothermometers yielded temperatures which agree well with the known downhole temperature. Also in agreement with these temperatures are the equilibrium reactions of calcite dissolution and bicarbonate-dissolved CO_2.
3. Corrosion coupon studies found generalized and uniform corrosion at rates of 10-15 mpy. One case of pitting was observed, which we attribute to increased dissolved O_2. An oxygen scavenger will be injected in future operations to minimize pitting corrosion. Scale deposition was minimal and did not affect operations.
4. Several periods of high dissolved CO_2 concentration, estimated at 1% by weight, created a temporary two-phase flow condition at a shallow depth in the production wellbore and in the surface loop. Future operations will require a gas separator to handle these transients.
5. Two radioactive tracer experiments resulted in modal volumes about twice as large as previous reservoirs at Fenton Hill. Furthermore, tracer recoveries are lower, indicating flow through a large number of fractures. The total swept fracture volume increased during this flow test as injected fluid continued to fill the reservoir. The total swept rock volume, calculated from tracer-determined fracture volumes and reasonable estimates of fracture porosity, is equivalent to a sphere of diameter equal to approximately the wellbore separation distance. This agreement lends credence to a point-source, point-sink model of flow through a network of fractures.

ACKNOWLEDGEMENTS

The authors thank George Cocks, Charles Grigsby, Motoyuki Inoue, Yoshihisa Shida, and Hideaki Kitamura for their assistance in collecting fluid and gas samples, and Joe Skalski, Lynn Brewer, and Bill Spurgeon for their help in setting up the sample collection equipment. Thanks also go to Hugh Murphy for reviewing this paper and to Cheryl Straub for typing the manuscript. This work was funded by the U.S. Department of Energy and the Government of Japan.

NOMENCLATURE

a^*	quartz surface area to fluid volume ratio (m^2/m^3)
b	fracture aperture (m)
C	concentration (kg/m^3)
C^*	dimensionless concentration in Eqn. (1)
C_{in}	injection fluid concentration (kg/m^3)
C_o	initial production fluid concentration (kg/m^3)
C^∞	silica saturation concentration (kg/m^3)
f_q	fraction of quartz present in granite
$f(V)$	residence time distribution curve (m^{-3})

k quartz dissolution rate constant (m/s)
K_{eq} equilibrium constant
K_H Henry's law constant (bar/mole fr.)
m_p mass of tracer injected (kg)
P pressure (bar)
P_{CO_2} partial pressure of CO_2 (bar)
P_w vapor pressure of water (bar)
t time (s)
V cumulative produced fluid volume (m^3)
x_{CO_2} mole fraction of CO_2
γ_i activity coefficient for component i
Φ dimensionless concentration in Eqn. (2)

REFERENCES

Hendron, R.H., "Fenton Hill Hot Dry Rock Overview", presented at the Twelfth Workshop on Geothermal Reservoir Engineering, Stanford University, Stanford, CA, Jan. 20-22 (1987).

Henley, R.W., Truesdell, A.H., and P.B. Barton, "Fluid-Mineral Equilibria in Hydrothermal Systems," Reviews in Economic Geology, V. 1 (1984).

Grigsby, C.O., "Rock-Water Interactions in Hot Dry Rock Geothermal Systems: Reservoir Simulation and Modeling," MS Thesis, Massachusetts Institute of Technology Dept. of Chemical Engineering (1983).

Grigsby, C.O., Tester, J.W., Trujillo, P.E., Counce, D.A., Abbott, J., Holley, C.E., and L.A. Blatz, "Rock-Water Interactions in Hot Dry Rock Geothermal Systems: Field Investigations of In Situ Geochemical Behavior," J. Volcan. and Geothermal Res., 15, 101-136 (1983).

Robinson, B.A., "Quartz Dissolution and Silica Deposition in Hot Dry Rock Geothermal Systems," MS Thesis, Massachusetts Institute of Technology Dept. of Chemical Engineering (1982).

Robinson, B.A., and J.W. Tester, "Dispersed Fluid Flow in Fractured Reservoirs: An Analysis of Tracer-Determined Residence Time Distributions," J. Geophys. Res., 89, B12, 10374-10384 (1984).

Trujillo, P.E., Counce, D., Grigsby, C.O., Goff, F., and L. Shevenell, "Chemical Analysis and Sampling Techniques for Geothermal Fluids and Gases at Fenton Hill Laboratory," Los Alamos National Laboratory internal report (1986).